

1 **Comment and discussion on “Scatterometer Hurricane Wind Speed Retrievals using Cross**
2 **Polarization, by G-J van Zadelhoff et al. ”**

3
4 Paul A. Hwang

5 Remote Sensing Division, Naval Research Laboratory, Washington DC, USA

6 paul.hwang@nrl.navy.mil

7
8 **1. INTRODUCTION**

9
10 As outlined in my review comments of the original manuscript:

11
12 The authors present their analysis of high wind retrieval using cross polarized radar
13 backscattering cross section (VH NRCS). From compiling 19 hurricane hunter missions of SFMR wind
14 measurements with RADARSAT-2 images, they are able to double the wind speed range from previous
15 reports. The relationship between VH NRCS and wind speed deviates significantly from previous
16 formulas for the wind range between 20 and 45 m/s. A new GMF is presented for this wind range.
17 Comparison study with numerical prediction (ECMWF) is also presented.

18
19 This is an interesting paper and obviously useful in new scatterometer development. There are
20 only a few minor points I would recommend the authors to clarify in their revision.

21
22 (1) The term “**linear**” [between VH NRCS and wind speed] is confusing (e.g., abstract: “The VH
23 backscatter has a linear relationship with respect to wind speed” as well as in many other places in the
24 text). The linear fit is between wind speed and VH NRCS in dB, so the VH NRCS (in physical unit of
25 backscattering cross section) increases exponentially with wind speed. This should be clarified in the
26 paper and the phrase “linear fit” needs to be used carefully.

27
28 (2) P9L22: “**One of the conclusions in literature was a lack of apparent incidence angle**
29 **dependence.**”: This statement is inaccurate. The incidence angle dependence is clearly illustrated from
30 theoretical computations (e.g., [Valenzuela 1967 IEEE TAPv15p552;] Hwang et al. 2010; Voronovich
31 and Zavorotny 2011 IGARSSp2033) and earlier analysis of a small RADARSAT-2 dataset (see Hwang
32 et al. 2010, Fig. 4b; Voronovich and Zavorotny 2011 Fig. 2). In fact, the empirical formula of Hwang et
33 al. (2010) incorporates the incidence angle factor (admittedly the result is not very good in high winds as
34 the formula was based on a much smaller dataset). The VH NRCS range as a function of incidence angle
35 shown in the present manuscript (Figs. 3 and 4) are consistent with those reported in the earlier
36 publications.

37
38 To stimulate discussion, here I expand on those two comments and extend analysis to the
39 directional distribution since the statement “**...the retrieval of wind direction ... is not possible for**
40 **the VH channel**” (van Zadelhoff et al., 2013, p. 7949) seems to be questionable at best and “**...that the**
41 **VH versus wind speed shows no dependence to the wind direction angles, as observed by Hwang**
42 **et al. (2010), ...**” (van Zadelhoff et al., 2013, p. 7959) is incorrect. The directional distribution was not
43 discussed in Hwang et al. (2010) “[b]ecause the sample size in each incidence angle bin is relatively
44 small for resolving directional distribution” (p. 4).

45

46 With regard to the incidence angle dependence in their published revision, the authors state that
47 “This [the incidence angle dependence] was also indicated by measurements using a limited set of
48 the RADARSAT-2 SCWA data (Hwang et al., 2010). The high signal-to-noise measurements from
49 the fine-quad polarization mode, however, showed a lack of apparent incidence angle dependence
50 (Vachon and Wolfe, 2011; Zhang and Perrie, 2011).” (p.7954). The data presented in Hwang et al.
51 (2010) are in fact from the fine-quad mode, this was clearly stated in their p. 3 (the first sentence of sec.
52 3).

53
54 I conclude with the suggestion for a more systematic analysis of the incidence angle and
55 azimuthal angle dependences in their next phase of data analysis in order to further improve the retrieval
56 algorithm of wind speed and direction using cross-pol radar backscatter.

57 58 2. RELEVANT PROPERTIES OF THE CROSS-POLARIZATION DATA

59 60 2.1. Incidence angle dependence

61
62 As outlined in Hwang et al. (2010b) [referred to as H10 from here on], the solutions of the co-pol
63 and cross-pol NRCS of a slightly rough patch tilted by the ocean surface have been summarized in
64 Valenzuela (1978). This surface scattering model is called tilted Bragg or composite-surface Bragg
65 scattering model (CB). The detail is given in sec. 2 of H10. The co-pol radar returns from RADARSAT-
66 2 (R2) show very good agreement with the CB model, the cross-pol is several dB higher than the CB
67 computation, as shown in Figs. 3 and 4 of H10, a simplified version is reproduced here as Fig. 1. For θ
68 between 22.5° and 37.5° , the calculated cross-pol difference is about 2 dB. The R2 data with wind speed
69 $U_{10} > \sim 5$ m/s, thus with higher signal to noise ratio (SNR), show a similar level of difference: for the
70 quad-pol data, the noise level is about -36 dB (Hwang et al., 2010a; Vachon and Wolfe, 2011), the
71 incidence angle dependence becomes especially clear for those data in Fig. 1c with $\sigma_{0HV} \geq \sim 30$ dB. For
72 R2 dual-pol mode, the cross-pol noise is about 5 to 6 dB higher than that of the quad-pol mode but the
73 incidence angle dependence remains quite noticeable (Hwang et al., 2010a, Fig. 2). The lower panels of
74 Figs. 3 and 4 in van Zadelhoff (2013) [referred to as vZ13 from here on] show a very similar range of
75 incidence angle variation in σ_{0HV} .

76 77 2.2. Wind speed dependence

78
79 As emphasized in H10, the most significant characteristics of σ_{0HV} , as far as wind speed
80 retrieval is concerned, is the increased sensitivity toward high wind and that the available cross-pol data
81 show no saturation in high winds. These are contrasted with the co-pol returns that may saturate at lower
82 incidence angles, as illustrated in the 22.5° data of Fig. 1 and the wind speed sensitivity obviously
83 decreases toward high wind. The much-larger dataset of vZ13 reconfirms those two very desirable
84 properties (increased sensitivity and unsaturation toward high wind). The clarification of the wind speed
85 dependence is especially valuable for improving our understanding of the backscattering mechanisms.
86 This is further explained next.

87
88 It is well known that the wind speed sensitivity of the Bragg resonance surface water waves
89 varies with the EM frequency. The ocean surface roughness spectral density can be expressed as a

90 power-law function $(u_* / c)^{a(k)}$, here u_* is the wind friction velocity, c is the phase speed of the
 91 roughness spectral component. The exponent a thus characterizes the wind speed sensitivity. For the
 92 microwave frequencies used in scatterometers, the sensitivity decreases from Ku to L band. In a recent
 93 study of the ocean surface roughness spectrum in high winds (up to 60 m/s) combining Ku, C and L
 94 band geophysical model functions (GMFs), Hwang et al. (2013) discover that the exponent of the power-
 95 law wind speed dependence of the Bragg resonance waves in those three frequency bands converges to
 96 0.75 in high winds ($u_* / c > 3$, or reference wind speed U_{10} greater than about 17 m/s for C band, note c
 97 has a minimum value of 0.23 m/s). For comparison, in mild to moderate wind speed the wind speed
 98 exponent is about 2 to 2.5 for Ku band, 1.2 to 1.5 for C band and 0.5 for L band (Fig.3 in Hwang et al.,
 99 2013). The dataset in vZ13 extends to 40 m/s wind speed and is of great interest.

100
 101 Figure 2 reproduces the VH GMF of vZ13:
 102

$$103 \quad \sigma_{0VH} (dB) = \begin{cases} 0.592U_{10} - 35.60, & U_{10} \leq U_t \\ 0.218U_{10} - 29.07, & U_{10} > U_t \end{cases} \quad (1)$$

104
 105 The transition wind speed U_t suggested by vZ13 is 21 m/s and the resulting curve has an obvious
 106 discontinuity (the green curve in Fig. 2a). The discontinuity is eliminated when the matching wind
 107 velocity of the two branches $U_t=17.46$ m/s is used (the blue solid curve in Fig. 2). The information of
 108 wind speed exponent can be better detected in a log-log plot. As illustrated in Fig. 2b, the cross-pol
 109 response to wind speed can be roughly divided into 4 different wind speed regions: (A) $U_{10} < 4$ m/s, the
 110 wind retrieval quality is low because of low SNR. The relatively-high background noise can be caused
 111 by sensor hardware as well as environmental factors such as swell and background turbulence
 112 contributing to ocean surface roughness that cannot be attributed to wind waves. (B) $4 \leq U_{10} < 10$ m/s, the
 113 SNR improves. The wind speed response is more or less linear, suggesting that the surface scattering as
 114 described in the CB model dominates the backscatter. As stated in the previous paragraph, for C band
 115 the CB model predicts wind speed exponent between about 1.2 and 1.5. (C) $10 \leq U_{10} < 18$ m/s, the cross-
 116 pol wind speed response is about quadratic, which is stronger than that of the Bragg waves. The
 117 enhanced wind speed sensitivity signifies the increasing influence of non-Bragg contributions
 118 attributable to wave breaking, which is expected to depend on wind speed cubed (e.g., Phillips 1985,
 119 1988; Hwang 2009). (D) $U_{10} \geq 18$ m/s, the wind speed exponent is about 1.5, which is twice of the C band
 120 Bragg wave wind speed exponent in high wind (0.75, see last paragraph) and again indicates the strong
 121 non-Bragg contribution of surface wave breaking.
 122

123 2.3. Azimuthal angle dependence

124
 125 As mentioned in the Introduction, the directional distribution was not discussed in H10 because
 126 the sample size in each incidence angle bin is relatively small for resolving directional distribution (H10,
 127 p4), and it is not accurate to state that “It is observed in the plot that the VH versus wind speed shows no
 128 dependence to the wind direction angles, as observed by Hwang et al. (2010), ...” (vZ13, p.7959).
 129

130 Here I present the directional analysis from those relatively small samples. Fig. 3 shows the
 131 results for the 20°-25° incidence angle bin and Fig. 4 shows the corresponding results for the 30°-35°

132 incidence angle bin. The quad-pol data are on the left column and the dual-pol on the right. The vertical
133 span of each plotting panel is identical (8 dB). It is evident that the directional signal of cross-pol is as
134 strong as or even stronger than those of the co-pols when SNR is good (quad-pol). Although the cross-
135 pol noise in the dual-pol product is about 5 to 6 dB higher than that of quad-pol, the cross-pol directional
136 signature in the dual-pol product remains significant.

137
138 From the point of view of scattering mechanisms, if surface effects dominate, then the cross
139 section (both co-pol and cross-pol) reflects the directional distribution of the ocean surface roughness.
140 Wave breaking also has strongly upwind-downwind asymmetry and will also contribute to cross-pol
141 azimuthal angle dependence in high winds. The authors correctly pointed out that L band cross-pol
142 shows distinctive directional dependence (Yueh et al., 2010). The side-by-side comparison shown in
143 Figs. 3 and 4 clearly indicates that the directional distributions of co-pol and cross-pol are comparable in
144 C band as well for good SNR data.

145 146 **3. CONCLUDING REMARKS**

147
148 The analysis reported in vZ13 represents a significant progress on the potential of cross-pol for
149 scatterometer applications, building upon the foundation of H10, Vachon and Wolfe (2011) and Zhang
150 et al. (2011). H10 emphasizes the significance of unsaturation of cross-pol returns in high winds for
151 ocean surface wind retrieval applications and foresees its contribution in future space monitoring of
152 damaging storms such as hurricanes. The analysis of vZ13 confirms that prediction. The cross-pol wind
153 retrieval algorithm presented in vZ13 makes use of the backscatter intensity alone. In an accompanying
154 paper (Belmont Rivas, Stoffelen and van Zadelhoff, 2013), the authors show that the addition of a single
155 VH capability in the mid beam of an ASCAT-type scatterometer improves the determination of wind
156 speed over the entire scatterometer swath, with wind speed RMS errors of about 0.5 m/s.

157
158 There are clear incidence angle and azimuthal angle dependences in the cross-pol return. The
159 incidence angle signal is relatively weak: about 2 dB between 22.5° and 37.5°. The directional signal, on
160 the other hand, is as strong as that of the co-pol returns (Figs. 3 and 4). Because of the weak cross-pol
161 return, instrument noise may compromise the directional signal somewhat but its presence remains
162 detectable. It is wonderful that retrieval of high wind speed using cross-pol achieves better results than
163 using co-pols without making use of the directional or incidence angle dependence, but it is incorrect to
164 state that the cross-pol signals do not vary with incidence angle or azimuthal angle. It would be a
165 mistake to write off C-band cross-pol as incapable of wind direction retrieval. Ultimately, the
166 unequivocal determination of the cross-pol directional distribution may require a circle flight or circular
167 scanning experiment similar to that performed by Yueh et al. (2010). In the meantime, side-by-side
168 comparison as shown in Figs. 3 and 4 suggests very similar directional distributions between co-pol and
169 cross-pol backscatters, and the co-pol directional distribution can be “borrowed” for cross-pol algorithm
170 development. The incidence angle and azimuthal angle dependences can and should be explored to
171 further enhance the performance of cross-pol wind vector retrieval.

172 173 **4. REFERENCES**

174
175 Belmont Rivas, M., Stoffelen, A., and van Zadelhoff, G.-J.: The benefit of HH and VH polarization in
176 retrieving extreme wind speeds for an ASCAT-type scatterometer, *IEEE Trans. Geos. Remote*

177 Sensing, in press, 2013.

178 Hwang, P. A., 2009: Estimating the effective energy transfer velocity at air-sea interface, *J. Geophys.*
179 *Res.*, 114, C11011, doi:10.1029/2009JC005497.

180 Hwang, P. A., Zhang, B., and Perrie, W.: Depolarized radar return for breaking wave measurement and
181 hurricane wind retrieval. *Geophys. Res. Lett.*, **37**, L01604, doi:10.1029/2009GL041780, 2010a.

182 Hwang, P. A., Zhang, B., Toporkov, J. V., and Perrie, W.: Comparison of composite Bragg theory and
183 quad-polarization radar backscatter from RADARSAT-2: with applications to wave breaking and
184 high wind retrieval, *J. Geophys. Res.*, 115, C08019, doi:10.1029/2009JC005995, 2010b.

185 Hwang, P. A., Burrage, D. M., Wang, D. W., and Wesson, J. C.: Ocean surface roughness spectrum in
186 high wind condition for microwave backscatter and emission computations, *J. Atmos. Oceanic Tech.*,
187 doi: 10.1175/JTECH-D-12-00239.1 (in press), 2013.

188 Phillips, O. M.: Spectral and statistical properties of the equilibrium range in wind-generated gravity
189 waves, *J. Fluid Mech.*, 156, 505-531, 1985.

190 Phillips, O. M.: Radar returns from the sea surface – Bragg scattering and breaking waves, *J. Phys.*
191 *Oceanogr.*, 18, 1065-1074, 1988.

192 Vachon, P. W., and Wolfe, J.: C-band cross-polarization wind speed retrieval, *IEEE Geos. Remote*
193 *Sensing Lett.*, 8, 456-458, 2011.

194 Valenzuela, G. R.: Depolarization of EM waves by slightly rough surfaces, *IEEE Trans. Antennas*
195 *Propag.*, 15, 552-557, 1967.

196 Van Zadelhoff, G.-J., Stoffelen, A., Vachon, P. W., Wolfe, J., Horstmann, J. and Belmonte Rivas, M.:
197 Scatterometer hurricane wind speed retrievals using cross polarization. *Atmos. Measure. Tech.*
198 *Discuss.*, 6, 7945-7984, 2013.

199 Voronovich, A. G., and V. U. Zavorotny: Depolarization of microwave backscattering from a rough sea
200 surface: Modeling with small-slope approximation, *Proc. Int. Symp. Geos. Remote Sensing*, 2003-
201 2036, 2011.

202 Yueh, S., Dinardo, S., Fore, A., and Li, F.: Passive and active L-band microwave observations and
203 modeling of ocean surface winds, *IEEE T. Geosci. Remote*, 48, 3087–3100,
204 doi:10.1109/TGRS.2010.2045002, 2010.

205 Zhang, B., Perrie, W., and He, Y.: Wind speed retrieval from RADARSAT-2 quad-polarization images
206 using a new polarization ratio model, *J. Geophys. Res.*, 116, C08008, doi:10.1029/2010JC006522,
207 2011.

208

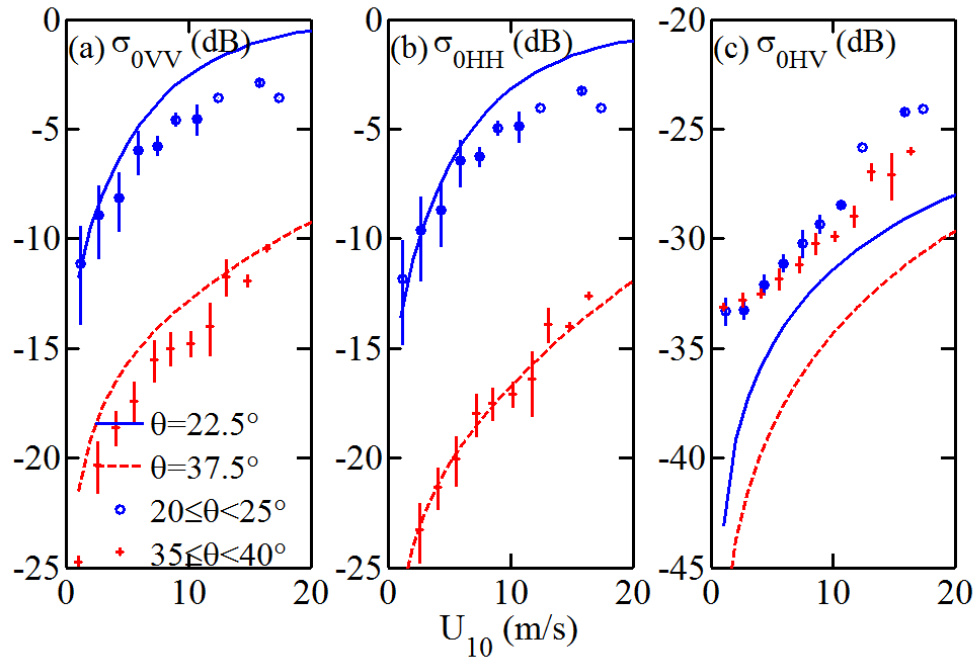


Fig. 1. Comparison of R2 quad-pol backscatters with composite-surface Bragg resonance model [adopted from Hwang et al. (2010b)].

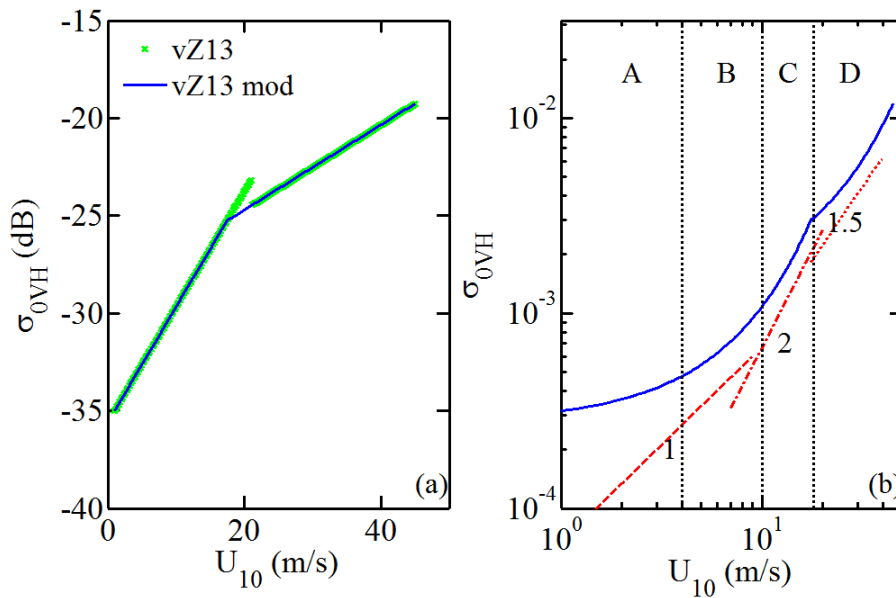


Fig. 2. Investigation of wind speed dependence based on the cross-pol GMF of van Zadelhoff et al. (2013). A modification of the transition wind speed at 17.4 (from 21) m/s is suggested for maintaining continuity.

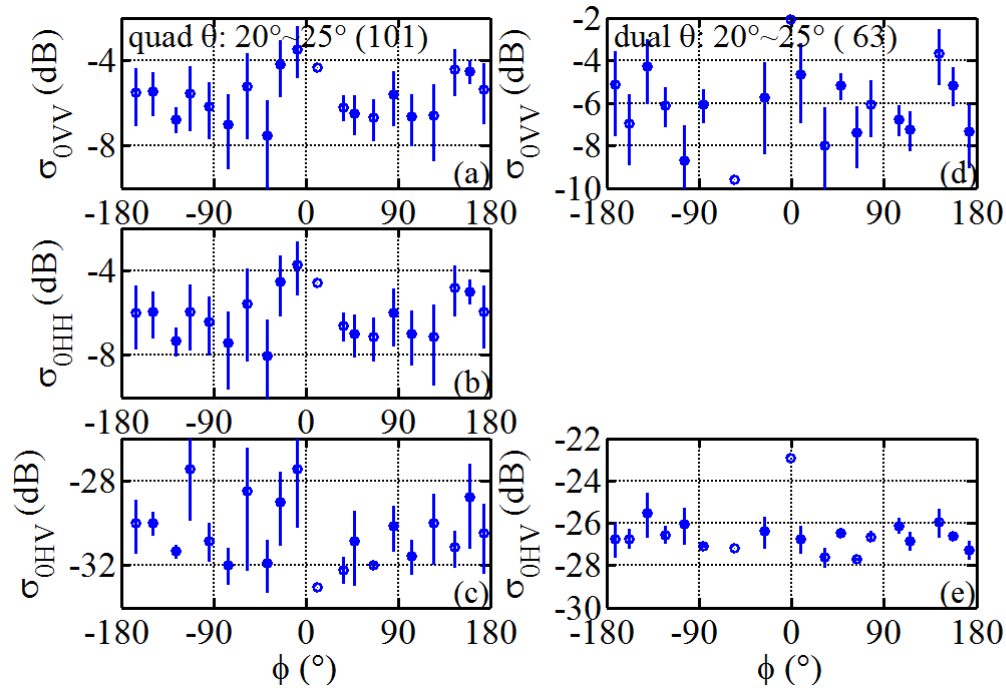


Fig. 3. Directional distribution of co-pol and cross-pol radar backscatters. Left column shows the R2 quad-pol results and the right column shows the dual-pol results. Incidence angle between 20° and 25° . The sample size is shown in parentheses of the top panels.

210

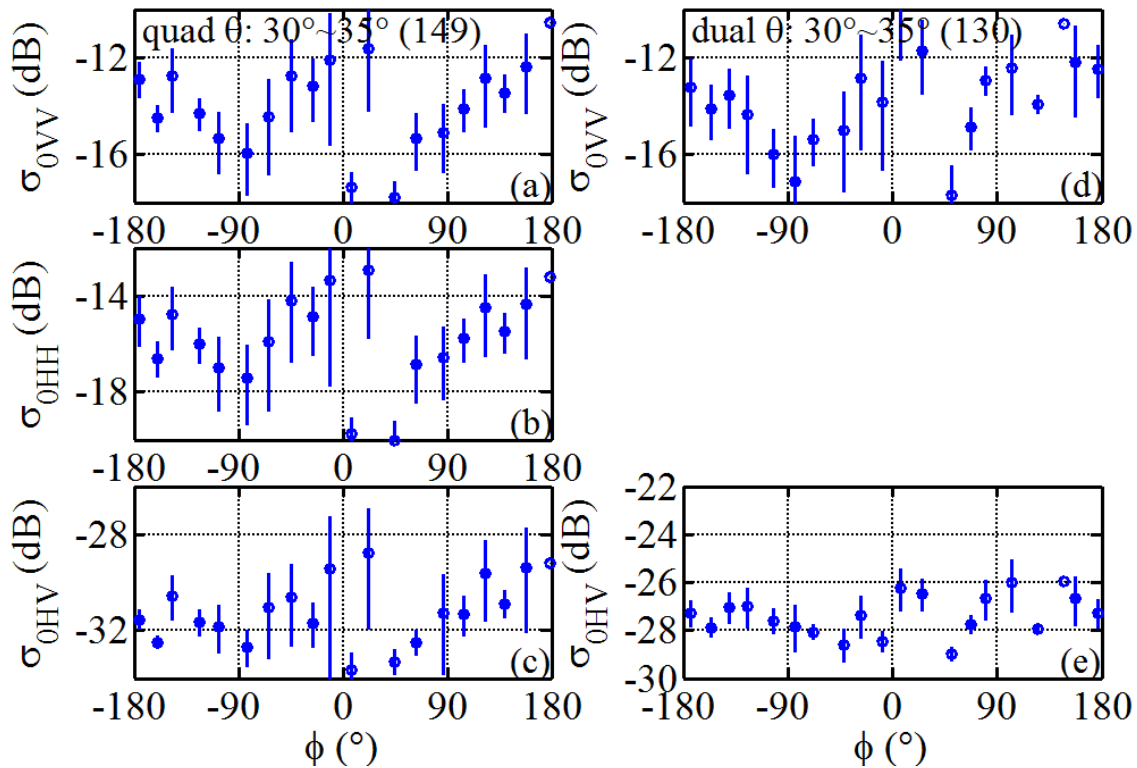


Fig. 4. Same as Fig. 3 but incidence angle between 30° and 35° .

211